Characteristics of Long Chain Branching in Ethene Polymerization with Single Site Catalysts

Anneli Malmberg,[†,‡] Jonas Liimatta,[†,⊥] Arja Lehtinen,[§] and Barbro Löfgren*[,†]

Polymer Science Centre, Helsinki University of Technology, Innopoli B2, P.O.Box 356, FIN-02151 Espoo, Finland, and Borealis Polymers Oy, P.O.Box 330, FIN-06101 Porvoo, Finland

Received May 5, 1999; Revised Manuscript Received July 30, 1999

ABSTRACT: Linear and long chain branched ethene homopolymers and copolymers with 1-hexene were produced with metallocene catalysts. The presence and absence of long chain branching in the polymers was studied by dynamic rheological and gel permeation chromatography−on-line viscometry analysis. Long chain branched polymers were produced with 1- and 2-siloxy-substituted derivatives of *rac*-Et(Ind)$_2$ZrCl$_2$/MAO and MeSi(C$_5$Me$_4$)(*N*-*t*-Bu)TiCl$_2$/MAO. As judged by the rheological behavior, *n*-ButCp$_2$ZrCl$_2$/MAO produced linear chains, as did the *meso* form of one of the substituted Et(Ind)$_2$ZrCl$_2$ catalyst structures. The rheological behavior of the polymers was affected by the polymerization conditions, especially by the addition of comonomer and the partial pressures of ethene and hydrogen. In addition, the slurry solvent was relevant to some of the catalysts. The effects of catalyst activity and different mass transfer limitations on the long chain branching were studied. As was evident from the rheological behavior, the long chain branching could be controlled by both the choice of the catalyst and the polymerization conditions. The rheological behavior is discussed with reference to the content of the long chain branches and the structure of the branching.

Introduction

The narrow molecular weight distribution that is characteristic of metallocene polymers is associated with desirable mechanical properties but poor material processability. Introducing long chain branching, while maintaining the narrow molecular weight and comonomer distribution, is desirable to enhance the pseudoplasticity (shear thinning) and melt elasticity of these polymers.

As regards single catalyst site systems, the ability to produce long chain branched polymer by copolymerization of vinyl-ended macromonomers with ethene has previously been attributed only to the dimethylsilylene-bridged amidocyclopentadienyltitanium complexes, i.e., the constrained geometry catalysts in solution processes.[1,2] Metallocene catalysts possess good copolymerization ability, produce vinyl-terminated chains, and have been shown to copolymerize long chain olefins.[1,3] They might, therefore, well produce long chain branching as well. Indeed, some very recent papers report rheological behavior indicating low levels of long chain branching (LCB) in polymers produced with conventional metallocene catalysts. Vega et al.[4,5] reported LCB behavior in ethene polymers produced with Cp$_2$ZrCl$_2$/MAO catalyst. Harrison et al.[6] reported behavior consistent with low levels of long chain branching in polymers prepared under slurry and gas-phase conditions with supported Et(Ind)$_2$ZrCl$_2$/MAO catalyst. Also, the patent literature[7] mentions the LCB behavior of polymers produced with supported Et(Ind)$_2$ZrCl$_2$/MAO in gas-phase polymerization.

In a previous paper,[8] we reported on the dynamic rheological behavior of ethene polymers synthesized with Et(Ind)$_2$ZrCl$_2$/MAO (EBIZ) and Et(IndH$_4$)$_2$ZrCl$_2$/MAO (EBH4IZ) catalysts. The EBIZ polymers exhibited a high complex viscosity at low frequency and steep frequency dependency of the complex viscosity, considerably higher than expected on the basis of the molecular weight and narrow MWD measured by gel permeation chromatography (GPC). The flow behavior of the EBH4IZ polymers was somewhat more moderate. The flow activation energy of both sets of polymers was elevated, the EBIZ polymers showing E_a values as high as LDPE and the EBH4IZ polymers showing somewhat lower values. Contents of long chain branching of 0.2/1000C were measured by ^{13}C NMR in a ethene homopolymer produced with EBIZ. Polymerization conditions affecting the rheology most were the partial pressure of ethene for EBIZ and the presence of hydrogen for EBH4IZ. We suggested the long chain branches in the polymers to be the result of copolymerization of vinyl-ended macromonomers with ethene.

Assuming different abilities of catalysts to incorporate vinyl-ended macromonomers in polymerization, one should expect differences in the amount and distribution of long chain branches in the polymers.[9,10] Branch architectures possible in copolymerization of vinyl-ended macromers with ethene can be described as comblike, treelike (dendritic), and star-shaped. The amount, length, and topology (distribution) of the long chain branches are difficult but interesting to assess. Another point of interest is the influence of the polymerization conditions on these features.

In this study, we explored the dynamic rheological and GPC−on-line viscometry behavior of metallocene catalyzed polymers. The polymers studied were ethene homopolymers and copolymers with 1-hexene, which were produced in laboratory-scale semibatch slurry polymerizations. The catalysts utilized were *n*-ButCp$_2$ZrCl$_2$/MAO, 1- and 2-siloxy-substituted variations of *rac*-Et(Ind)$_2$ZrCl$_2$/MAO,[11,12] and MeSi(C$_5$Me$_4$)(*N*-*t*-Bu)TiCl$_2$/MAO. As judged by the rheological behavior, *n*-ButCp$_2$ZrCl$_2$/

† Helsinki University of Technology.
‡ Current address: Borealis Polymers Oy, P.O. Box 330, FIN-06101 Porvoo, Finland.
§ Borealis Polymers Oy.
⊥ Current address: Fortum Oil and Gas Oy, P.O. Box 310, FIN-06101 Porvoo, Finland.

10.1021/ma9907136 CCC: $18.00
Published on Web 09/18/1999

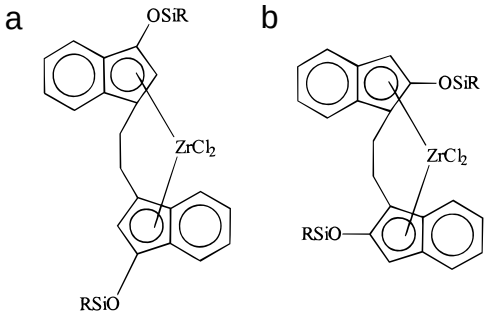

Figure 1. Generic structure of the 1- (a) and 2-siloxy-substituted (b) *rac*-Et(Ind)$_2$ZrCl$_2$ complexes.

MAO produced linear chains. Like Et(Ind)$_2$ZrCl$_2$/MAO, its siloxy-substituted derivatives produced long chain branched polymers, and so did MeSi(C$_5$Me$_4$)(*N*-*t*-Bu)-TiCl$_2$/MAO. Interestingly, the correlation between MFR$_{21}$, the GPC-measured molecular weight and the complex viscosity seemed to be virtually unique for each catalyst. Besides the choice of catalyst, the polymerization conditions—ethene pressure, presence of hydrogen and comonomer and even the polymerization solvent—affected the rheological behavior. We discuss these various factors in terms of amount and distribution (architecture) of the long chain branching obtained in the polymers.

Experimental Section

Polymerization. The metallocene catalysts were *n*-ButCp$_2$-ZrCl$_2$ (Cat 1) and three siloxy-substituted[11,12] derivatives of *rac*-Et(Ind)$_2$ZrCl$_2$, differing in size and position of the siloxy group. Cat 2 bore the siloxy substitute in 2-position of the indenyl ring, whereas the siloxy group was in the 1-position in catalysts 3 and 4. Figure 1 shows the structure of the siloxy-substituted catalysts. In addition, the *meso* form of one of the catalysts (*meso*-Cat 2) and MeSi(C$_5$Me$_4$)(*N*-*t*-Bu)TiCl$_2$ (Cat 5) were tested.

The polymers were synthesized in semibatch laboratory-scale slurry polymerizations at 80 °C with either pentane or toluene as the solvent. All catalysts were activated with MAO, the ratio Al/Zr being 1000. Hydrogen and the comonomer 1-hexene were fed batchwise before the catalyst was injected. During polymerization, the ethene flow was adjusted so as to maintain the desired polymerization pressure. Where pentane provided the solvent, the solvent and residual monomers were evaporated after polymerization. In the case of toluene, the polymer was precipitated with EtOH/HCl and washed with EtOH and dried in a vacuum. The polymer powders were milled and stabilized with 2000 ppm of antioxidant.

Polymer Characterization. FTIR and NMR measurements were made to study the polymer composition and double bond containing end groups. ^{13}C NMR spectra were recorded on a Varian XL-300 NMR spectrometer operating at 75 MHz at 125 °C. The pulse angle was 60°, acquisition time 1.8 s, and pulse delay 6.0 s. The carbon signals were assigned according to Randall.[13] A Nicolet Magna FTIR was used to determine the comonomer content after calibration against ^{13}C NMR results. The double bond determination was carried out on 0.5 mm melt-pressed disks using the method of Haslam et al.[14] Antioxidant was found to disturb the regions of interest in the IR spectra, so unstabilized polymer was used in the IR analysis.

The apparent molecular weights (M_w and M_n) and molecular weight distribution (MWD) were determined on a Waters 150C high-temperature GPC instrument equipped with a refractometer detector. The GPC was calibrated with narrow MWD polystyrene standards that covered the molecular weight region from 10^3 to 10^7. In addition to this, well-characterized polyethene samples were used as in-house standards. The samples were dissolved in trichlorobenzene and the measurement was carried out at 135 °C. The GPC−on-line viscometry (GPC−OLV) measurements were carried out at 135 °C using a Waters 150cvplus instrument equipped with both refractometer index (RI) and intrinsic viscosity detectors. The weight-averaged sum of intrinsic viscosities at each point along the chromatogram equals the sample intrinsic viscosity. Branching index $g' = [\eta]_{branched}/[\eta]_{linear}$. The melt flow rates were determined at 190 °C according to ASTM method D 1238.

Dynamic Rheological Measurements. The samples were stabilized for the rheological measurements with 2000 ppm Irganox B 215 antioxidant. After stabilization, the samples were melt pressed at 190 °C into 1 mm thick disks using a Fontijne TP 400 table press. The viscoelastic behavior was studied with a stress controlled dynamic rheometer SR-500 manufactured by Rheometric Scientific. The dynamic measurements were then run with a 25 mm plate and plate geometry and a 1 mm sample gap. The frequency dependence of the moduli was determined with frequencies from 0.02 to 100 rad/s, using strain values determined with a stress sweep to lie within the linear viscoelastic region. Measurements were carried out in nitrogen atmosphere at three different temperatures between 150 and 210 °C. Rheometrics RSI Orchestrator software was used to shift the moduli curves along the frequency axis with compensation for the effect of temperature on melt density to construct the master curves and to determine the shift factor a_T. The shift factors were then plotted against $1/T$ to obtain the Arrhenius-type flow activation energy E_a. Only correlation factor R2 values greater than 0.99 were accepted in the line fit.

Thermal stability of the samples during the rheological testing was checked by repeating one low-frequency measurement point after the primary frequency sweep. In no sample was the change in storage modulus G' during the frequency sweep greater than 5%. The thermal stability of selected polymers was also studied in a separate time sweep, where the polymers gave a stable G' signal for at least 90 min at 190 °C. In addition, some samples were analyzed by FT-IR and GPC after the rheological analysis. Changes in the double bond pattern were within the range of test reproducibility, and no changes were noted in the molecular weight distribution curve. This allows us to conclude that no chain extension or cross-linking of the chains occurred during the rheological measurements. The unwashed polymers had ash content of 0.08 wt %. To check whether the catalyst residues affected the polymer relaxation behavior, selected polymer samples were dissolved in boiling xylene. The polymers were precipitated with EtOH, dried, and restabilized, and their viscoelastic behavior was studied. Essentially similar viscoelastic behavior as obtained with unwashed samples was seen.

Rheology Reference Materials. The rheological behavior of the experimental materials was compared with that of commercial polyolefins. The LDPE reference sample was characterized by high molecular weight, broad molecular weight distribution, and a flow activation energy of 50 kJ/mol, typical for low-density polyethene. The LLDPE sample was a conventional Ziegler−Natta catalyzed film-grade linear low-density polyethene, M_w 80 000 and MWD 4.0, yielding 33 kJ/mol for flow activation energy. The Cr−HDPE sample was a chromium-catalyzed high-density grade polyethene with few or no long chain branches, characterized by high molecular weight (M_w 300 000) and broad MWD (15). The flow activation energy of this material was 31 kJ/mol.

Results and Discussion

In the following section, polymer samples are numbered so that the first digit indicates the catalyst used in the preparation. Thus, polymer 11 is sample 1 prepared with catalyst 1 and polymer m21 is sample 1 prepared with the *meso* form of catalyst 2.

Complex Viscosity of the Melt and GPC Molecular Weights. Figure 2a shows the frequency dependence of the complex viscosity of the polymer melts. For

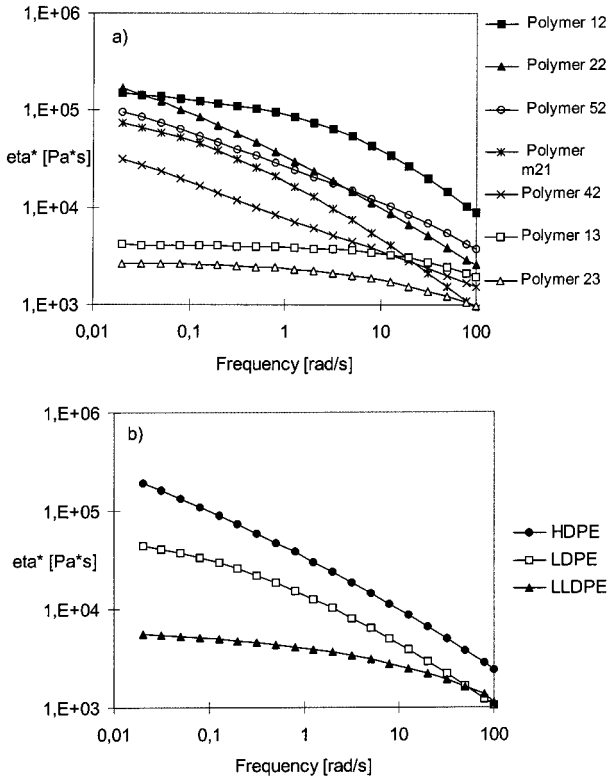

Figure 2. Frequency dependence of the complex viscosity of polymer melts at 190 °C. An asterisk indicates M_w and MWD obtained by GPC−OLV analysis; otherwise they are obtained by GPC: (a) Cat 1 polymer 12, M_w 300 000 and MWD 2.5; polymer 13, M_w 110 000 and MWD 2.3. Cat 2 polymer 22, M_w 170 000 and MWD 3.9*; polymer 23, M_w 106 000, MWD 3.8*. *meso*-Cat 2 polymer m21, M_w 235 000 and MWD 17. Cat 4 polymer 42, M_w of 135 000, MWD 9.0*. Cat 5 polymer 52, M_w 185 000, MWD 3.7*. (b) Behavior of commercial polyethenes, a Cr-catalyzed HDPE (M_w 300 000, MWD 17), a radical polymerized LDPE, and Z−N-catalyzed LLDPE (M_w 100 000, MWD 4).

comparison, Figure 2b shows the behavior of three commercial polyethenes, a Cr-catalyzed HDPE, a radical-polymerized LDPE, and a Z−N-catalyzed LLDPE. A comparison of the low frequency complex viscosities plotted in Figure 2 with the molecular weights measured by GPC reveals some discrepancies between the rheological behavior and the molecular weight data. Only Cat 1 and *meso*-Cat 2 produced polymers with the rheological behavior expected on the basis of their molecular weight and MWD. The complex viscosity of the unbridged Cat 1 polymers 12 (high M_w of 300 000) and 13 (low M_w of 110 000) was shear rate independent at low frequencies and showed little shear thinning, as expected for a polymer with narrow MWD (M_w/M_n = 2.3 and 2.2). The complex viscosity curve of *meso*-Cat 2 polymer m21 (high M_w of 235 000) showed early onset of the increasing shear thinning behavior, as would be expected for a broad MWD, 17.

In comparison to these polymers, the complex viscosity at lowest frequencies of polymers polymerized with the EBIZ catalyst variations Cat 2 and Cat 4 (polymers 22 and 42) and dimethylsilylene-bridged amidocyclopentadienyltitanium complex Cat 5 (polymer 52) was higher or even much higher than expected on the basis of the measured molecular weight. Moreover, the complex viscosity exhibited a sharp shear rate dependence. In GPC−OLV analysis, sample 22 exhibited a M_w of 170 000, sample 42 a M_w of 135 000 and sample 52 a

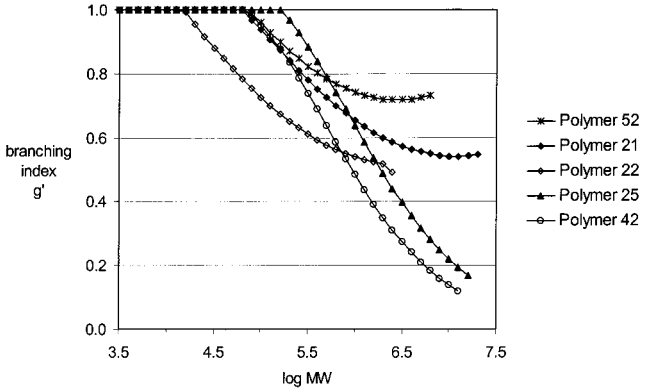

Figure 3. Branching index g' as a function of molecular weight obtained from GPC−on-line viscometry analysis. Polymers were produced with catalysts 2, 4, and 5.

M_w of 185 000. Molecular weight distributions obtained in the GPC analysis were unimodal: MWD = 3.9 for polymer 22, 9.0 for polymer 42, and 3.7 for polymer 52. This discrepancy between the complex viscosity and the GPC results indicates the presence of species with high relaxation times in the Cat 2, Cat 4, and Cat 5 polymers.

In an attempt to understand the discrepancy, selected polymers were studied by GPC with dual detectors, i.e., GPC−on-line viscometry (GPC−OLV) and GPC−light scattering (GPC-LS). In solution, branched polymers assume a more compact configuration than do linear chains, and thus long chain branched polymers may yield too low molecular weights in conventional GPC analysis. GPC with dual detectors improves the sensitivity toward high molecular weights.[15,16] In addition, information on the branching along the MWD can be obtained. The branching index g' obtained from GPC−OLV as $g' = [\eta]$branched/ $[\eta]$linear is often used as a measure of long chain branching.[17] It is likely that the hydrodynamic volume occupied by a branched molecule in solution also depends on the amount and type of the long chain branching. A further point to consider, therefore, is the structural homogeneity of the polymers produced in the polymerization process.

As shown in the tables, the GPC−OLV M_w values of the samples were not appreciably higher than the conventional GPC values. The same was true for the GPC−LS values: for polymer EBIZ6, GPC analysis gave M_w of 140 000 and GPC−MALS 180 000. The molecular weight distribution curves recorded by GPC−OLV and conventional GPC were of similar unimodal shape. The values of the branching index g' obtained from GPC−OLV were only slightly lowered relative to the value of 1 for linear polymers. The values ranged from 1 to 0.65, whereas for long chain branched LDPE g' can be as low as 0.3. Figure 3 shows the branching index g' as a function of the molecular weight obtained from GPC−OLV measurements for catalyst 2, 4, and 5 polymers. The solution viscosity of the polymers starts to deviate from that of a linear polymer at molecular weights above 10 000. The Cat 2 polymer 25 and Cat 4 polymer 42 exhibit a much steeper decrease in g' than the Cat 5 polymer 52. The decrease is also steeper for Cat 2 polymer 25, which was polymerized at 5 bar of ethene partial pressure, than for the polymer 21, which was polymerized at 10 bar.

In line with the deviation reported by Vega et al.[5] for Cp_2ZrCl_2-catalyzed polymers, we note that the low-frequency complex viscosity of the dimethylsilylene-bridged amidocyclopentadienyltitanium complex and

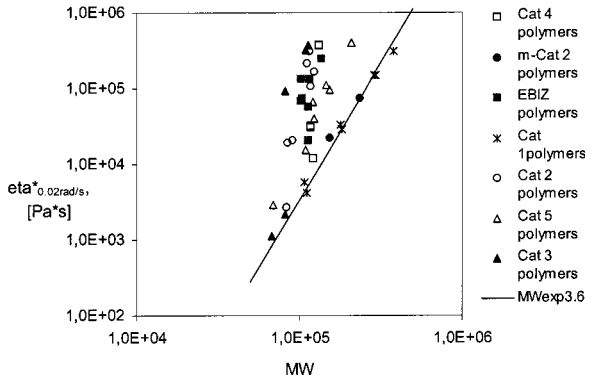

Figure 4. GPC−weight-average molecular weight dependence of the value of complex viscosity η^* at $\omega = 0.02$ rad/s at 190 °C. The line corresponds to log $\eta = 3.3 \times 10^{-15} \times M_w^{3.6}$. [18]

EBIZ-type catalyst polymers did not follow the 3.6 power dependence of M_w well established for linear polymers.[18] As can be seen in Figure 4, only the Cat 1 and *meso*-Cat 2 materials followed the 3.6 power dependence. The other materials deviate upward from the line, in increasing degree as the molecular weight increases. The results speak for long chain branching in polymers produced with the EBIZ based catalysts 2, 3, and 4, and with the amidocyclopentadienyltitanium catalyst, Cat 5. That the presence of ultrahigh molecular weight linear species in the polymers would be the sole cause of the high complex viscosity at low frequency does not seem likely, given the complexity in thermorheological behavior and the influence of the polymerization conditions on it. These points are discussed in the following section.

Thermorheological Complexity. Long chain branches have a strong influence on the melt behavior owing to their influence on the chain relaxation. Whereas linear chains relax by reptation of the entire chain, branch points constrain the motion of a long chain branched polymer and relaxation requires additional, slower processes as well.[19] This results in a broadened relaxation spectrum.[20] The effect is seen as enhanced melt viscosity at low shear rates. In peroxide randomly cross-linked polyethene, a low amount of peroxide (low content of branches) has been found to enhance the viscosity markedly,[21,22] but at higher peroxide (and branch) content, the viscosity is lowered. This decrease is explained in terms of a decrease in the molecule size.[23] In narrow MWD model three-arm star polybutadienes, viscosity increases with arm length.[24,25] As discussed by Vega et al.,[5] the peroxide cross-linked polyethenes and star-shaped polybutadienes differ in their branching distribution. The cross-linked polyethene is randomly branched—in fact it is a blend of linear and (a small portion) branched molecules—whereas the star polybutadienes contain exactly one branch point per molecule.

Reflecting the different relaxation mechanisms, the longest relaxation times in long chain branched polymers are more temperature dependent than the short relaxation times.[24] This is readily seen in the temperature dependence of the viscoelastic properties of ethene polymers.[26] In the model, narrow MWD three-arm polybutadienes, the flow activation energy E_a increases with arm length, and in blends of linear and star-shaped polybutadienes, it increases with the volume fraction of the star polymer.[25] In peroxide cross-linked polyethenes,[23,27] E_a increases with the content of branches (peroxide level). Unfortunately, the increasing complexity of the structure by long chain branching also manifests itself as departures from the time−temperature superposition and this leads to thermorheologically complex behavior: the shape of the modulus−frequency curve changes with temperature, and the calculated activation energy becomes stress (modulus) dependent.[26,28]

The rheology reference samples were selected to vary both in their molecular weight and in structure, from linear to branched. Thus, an E_a of 30 kJ/mol was derived for the Cr−HDPE sample, 33 kJ/mol for the LLDPE sample, and 55 kJ/mol for the LDPE sample. All these values are in line with reported values.[28,29] For single-site-catalyzed, controlled long chain branched polyethenes, Kim et al.[30] report E_a values ranging from 33 to 39 kJ/mol, based on data from capillary rheometry. Hatzikiriakos et al.[31] recently reported 40 and 45 kJ/mol for constrained geometry catalyst materials, calculated on the basis of dynamic rheological data. Vega et al.[4,5] reported values from 30 to 40 kJ/mol for ethene polymers polymerized with Cp_2ZrCl_2/MAO catalyst. In linear polymers, E_a increases with the comonomer level. In estimating the LCB level from the rheology, the effect of comonomer on the E_a should be taken into account.[5,32]

We obtained a value of 26 kJ/mol for the flow activation energy of the *n*-butCp_2ZrCl_2/MAO (Cat 1) polymer 11, which we consider to represent a chain with a linear HDPE-type structure[29] (Table 1). For the bridged metallocene catalyst polymers, calculated values of flow activation energy ranged from 30 kJ/mol (Cat 1, *meso*-Cat 2) and 38 kJ/mol (Cat 5, Cat 4) to values equal to those of LDPE, over 50 kJ/mol (EBIZ, Cat 2). Through comparison with literature values for LDPE, LLDPE, and HDPE, we interpret these values to indicate moderate to substantial degrees of long chain branching. However, as reported in our previous paper,[8] ^{13}C NMR indicated a branch content of only 0.2 branches per 1000C in a homopolymer with the EBIZ catalyst, which exhibited high flow E_as of over 50 kJ/mol. In ^{13}C NMR and under the same conditions as earlier, we failed to detect LCB in the present polymers. Thermorheologically complex behavior was nevertheless clearly present. The temperature shift of the modulus curves on the frequency scale increased with decreasing modulus, which is a clear indication of thermorheological complexity and long chain branching. Although this finding further provides evidence for the LCB structure of the polymers, it also induces uncertainty in the E_a values that were obtained: the higher the values the more the uncertainty. For most of the polymers, the experimentally accessible rheological data did not extend close to the most informative, terminal region of the viscoelastic behavior. Although performing the shift may be a somewhat doubtful procedure when behavior is obviously complex, we did this to obtain a tool for comparing the catalysts.

As seen in Tables 2a, 4, 5, and 6, the presence of hydrogen in the polymerization reduced the amount of vinyl bonds, the molecular weight, the complex viscosity and the flow E_a, but the degree of reduction depended on the catalyst. Compare, for example, the slight differences in EBIZ polymers EBIZ3 (no H_2) and EBIZ5 (H_2 present) with the marked differences in the Cat 2 polymers 21 (no H_2) and 23 (H_2 present). (The complex viscosity curves of polymers 21 and 23 were shown in Figure 2a.) In a similar way, the (*n*-but$Cp)_2ZrCl_2$ and Et$(IndH_4)_2ZrCl_2$ polymers revealed strong sensitivity of

Table 1. Characteristics of Polymers Produced with Cat 1

				FT-IR					GPC		dynamic rheology		
					double bond pattern, %								
polymer[b]	p_E, bar	H_2/Zr	yield, g	comon wt %	*trans*-v[a]	vinyl[a]	vdene[a]	MFR_{21}, g/10 min	$10^{-3}M_w$	MWD	$\eta_{0.02rad/s}$(190 °C), Pa s	$G'_{(G''2000)}$, Pa	E_a, kJ/mol
11[c]	3	0	9	0	n.m.[e]	n.m.	n.m.	n.m.	380	2.2	307 000	*f*	26
12[c,d]	5	0	60	1.2	n.m.	n.m.	n.m.	n.m.	300	2.2	150 000	*f*	27
13	5	0	200	0	n.m.	n.m.	n.m.	24	110	2.3	5810	140	30
14[d]	5	0		4.1	39	42	19	28	110	2.3	4140	92	35

[a] Measured from *trans*-vinylene absorbance at 965 cm^{-1}, vinyl at 910 cm^{-1}, and vinylidene at 888 cm^{-1}. [b] Polymerization: 0.5×10^{-6} mol of catalyst, Al/Zr 1000, polymerization time 60 min at 80 °C, 1.8 L of pentane. [c] In toluene, 1×10^{-6} mol of catalyst. [d] 15 mL of 1-hexene. [e] n.m.: not measured. [f] No value.

Table 2. Characteristics of Polymers Produced with Cat 2 and *meso*-Cat 2

				FT-IR					GPC		GPC−OLV		dynamic rheology		
					double bond pattern, %										
polymer[b]	p_E, bar	H_2/Zr	yield, g	comon wt %	*trans*-v[a]	vinyl[a]	vdene[a]	MFR_2, g/10 min	$10^{-3}M_w$	MWD	$10^{-3}M_w$	MWD	$\eta_{0.02rad/s}$(190 °C), Pa s	$G'_{(G''2000)}$, Pa	E_a, kJ/mol
(a) Cat 2															
21	10	0	120	0	0	98	2	11	110	2.7	150	4.0	107 000	990	48
22[c]	10	0	166	1.1	0	94	6	6.3	120	2.6	170	3.9	168 000	*g*	53
23[c,d]	10	13 700	113	1.7	4	73	23	81	83	2.9	105	3.8	2670	235	30
24[e]	10	0	159	1.9	0	98	2	29	120	3.0	n.m.[f]	n.m.	57 000	1140	43
25	5	0	66	0	0	98	2	9.1	110	2.5	150	4.0	217 000	*g*	57
26[c]	5	0	97	2.5	0	90	10	36	91	2.2	125	3.3	20 700	710	44
27	2.5	0	50	0	0	95	5	1.2	160	3.2	205	4.8	n.m.	n.m.	n.m.
28[c]	2.5	0	41	3.1	8	76	16	11	115	2.8	n.m.	n.m.	315 000	*g*	n.m.
(b) *meso*-Cat 2															
m21	10	0	156	0	0	95	5	68	240	16.8	220	25	73 900	805	30
m22[c]	10	0	200	1.7	0	90	10	170	150	10.6	n.m.	n.m.	22 400	915	33
m23	2.5	0	28	0	2	91	7	81	170	10.7	n.m.	n.m.	81 100	1700	n.m.
m24[c]	2.5	0	28	4.7	1	83	16	460	78	4.2	n.m.	n.m.	n.m.	n.m.	n.m.

[a] Measured from *trans*-vinylene absorbance at 965 cm^{-1}, vinyl at 910 cm^{-1}, and vinylidene at 888 cm^{-1}. [b] Polymerization: 0.3×10^{-6} mol of catalyst, cocatalyst MAO, Al/Zr 1000, polymerization time 30 min at 80 °C, 1.8 L of pentane. [c] 25 mL of 1-hexene. [d] Polymerization time 15 min. [e] In toluene. [f] n.m.: not measured. [g] No value.

Table 3. Characteristics of Polymers Produced with Cat 3

				FT-IR					GPC		dynamic rheology		
					double bond pattern, %								
polymer[b]	p_E, bar	H_2/Zr	yield, g	comon wt %	*trans*-v[a]	vinyl[a]	vdene[a]	MFR_2, g/10 min	$10^{-3}M_w$	MWD	$\eta_{0.02rad/s}$(190 °C), Pa s	$G'_{(G''2000)}$, Pa	E_a, kJ/mol
31	10	0	73	0	9	91	0	112	67	2.0	1120	140	26
32[c]	10	0	200	5.5	0	58	42	9.2	110	3.2	324000	$G' > G''$	n.m.[e]
33	2.5	0	24	0	0	95	5	65	82	2.0	2150	170	27
34[d]	2.5	0	17	7.2	6	57	37	12	110	2.8	369000	$G' > G''$	n.m.

[a] Measured from *trans*-vinylene absorbance at 965 cm^{-1}, vinyl at 910 cm^{-1}, and vinylidene at 888 cm^{-1}. [b] Polymerization: 0.3×10^{-6} mol of catalyst, cocatalyst MAO, Al/Zr 1000, polymerization time 30 min at 80 °C, 1.8 L of pentane. [c] 50 mL of 1-hexene. [d] 25 mL of 1-hexene. [e] n.m.: not measured. [f] no value.

Table 4. Characteristics of Polymers Produced with Cat 4

				FT-IR					GPC		GPC−OLV		dynamic rheology		
					double bond pattern, %										
polymer[b]	p_E, bar	H_2/Zr	yield, g	comon wt %	*trans*-v[a]	vinyl[a]	vdene[a]	MFR_2, g/10 min	$10^{-3}M_w$	MWD	$10^{-3}M_w$	MWD	$\eta_{0.02rad/s}$(190 °C), Pa s	$G'_{(G''2000)}$, Pa	E_a, kJ/mol
41	5	16 400	65	0	7	80	13	33	120	5.5	n.m.[e]	n.m.	32 300	1075	n.m.
42	5	16 400	90	0	3	83	13	27	120	4.8	135	9.0	31 000	1240	38
43[c]	5	16 400	83	6.7	2	54	44	11	130	3.7	160	6.5	373 000	$G' > G''$	n.m.
44[d]	5	0	89	0	15	80	5	15	120	2.0	n.m.	n.n.	11 900	130	28

[a] Measured from *trans*-vinylene absorbance at 965 cm^{-1}, vinyl at 910 cm^{-1}, and vinylidene at 888 cm^{-1} [b] Polymerization: 0.25×10^{-6} mol of catalyst, cocatalyst MAO, Al/Zr 1000, polymerization time 15 min at 80 °C, 1.8 L of pentane. [c] 25 mL of 1-hexene. [d] In toluene. [e] n.m.: not measured. ** no value.

the catalyst to H_2,[33] while $Et(Ind)_2ZrCl_2$ (EBIZ) was only mildly sensitive.[8] Relatively large amounts of H_2 also had to be used with Cat 5 to achieve lower values.

In line with the findings of Suhm et al.,[34] the dimethylsilylene-bridged amidocyclopentadienyltitanium catalyst, Cat 5 exhibited good copolymerization ability, but in comparison with the other catalysts much lower polymerization activity. Catalysts 3 and 4 showed very good comonomer response.

Lowering the ethene concentration favored the comonomer incorporation (e.g., polymers 22, 26, and 28), and a similar trend in macromonomer insertion could occur. In fact, at very low ethene pressures, we observed[33] a steady increase of complex viscosity and flow E_a with decreasing ethene pressure when $Et(Ind)_2ZrCl_2$/MAO served as the catalyst. The same effect on a milder scale was seen in the Cat 2 homopolymers. The low-frequency complex viscosity of polymer 25 (polymerized at 5 bar

Table 5. Characteristics of Polymers Produced with Cat 5

				FT-IR									dynamic rheology		
					double bond pattern, %				GPC		GPC−OLV				
polymer[b]	p_E, bar	H_2/Zr	yield, g	comon wt %	*trans*-v[a]	vinyl[a]	vdene[a]	MFR_2, g/10 min	$10^{-3}M_w$	MWD	$10^{-3}M_w$	MWD	$\eta_{0.02rad/s}$(190 °C), Pa s	$G'_{(G''2000)}$, Pa	E_a, kJ/mol
51	10	0	42	0	0	100	0	n.m.[d]	n.m.	n.m.	n.m.	n.m.	n.m.	n.m.	n.m.
52	10	2000	55	0	0	69	31	6.7	150	2.5	185	3.7	96 300	955	38
53[c]	10	2000	74	3.4	0	63	37	9.0	150	2.6	n.m.	n.m.	111 000	1000	37
54[c]	10	2000	111	3.3	0	60	40	3.1	210	2.8	n.m.	n.m.	396 000	*e*	38
55[c]	10	0	30	5.5	3	46	51	n.m.	n.m.		n.m.	n.m.	n.m.	*e*	n.m.
56[c]	5	2000	106	5.1	0	63	37	98	69	2.1	90	3.0	2900	420	n.m.

[a] Measured from *trans*-vinylene absorbance at 965 cm^{-1}, vinyl at 910 cm^{-1}, and vinylidene at 888 cm^{-1} [b] Polymerization: 5×10^{-6} mol of catalyst, cocatalyst MAO, Al/Zr 1000, polymerization time 60 min at 80 °C, 1.8 L of pentane. [c] 25 mL of 1-hexene. [d] n.m.: not measured. [e] No value.

Table 6. Characteristics of Polymers Produced with EBIZ ($Et(Ind)_2ZrCl_2$/MAO) Catalyst with Data from Ref 8

				FT-IR									dynamic rheology		
					double bond pattern, %				GPC		GPC−OLV				
polymer[b]	p_E, bar	H_2/Zr	yield, g	comon wt %	*trans*-v[a]	vinyl[a]	vdene[a]	MFR_2, g/10 min	$10^{-3}M_w$	MWD	$10^{-3}M_w$	MWD	$\eta_{0.02rad/s}$(190 °C), Pa s	$G'_{(G''2000)}$, Pa	E_a, kJ/mol
EBIZ1	10	0	132	0	3	94	3	21	110	3.2	160	5.0	58 600	965	48
EBIZ2[c]	10	0	109	2.0	3	87	10	21	100	2.7	150	4.3	68 500	920	53
EBIZ3	5	0	57	0	7	89	4	7.2	140	3.3	170	4.0	251 000	*e*	51
EBIZ4[c]	5	0	74	3.0	7	80	13	15	115	2.8	180	5.1	136 000	*e*	56
EBIZ5	5	8300	54	0	0	93	7	19	100	3.7	130	7.0	132 000	*e*	59
EBIZ6	2.5	0	14	0	6	87	6	2.2	140	3.0	220	5.5	n.m.[d]	n.m.	n.m.
EBIZ7[c]	2.5	0	74	5.5	9	73	18	32	110	3.2	135	4.5	20 800	340	48

[a] Measured from *trans*-vinylene absorbance at 965 cm^{-1}, vinyl at 910 cm^{-1}, and vinylidene at 888 cm^{-1}. [b] Polymerization: 0.5×10^{-6} mol of catalyst, Al/Zr 1000, polymerization time 60 min at 80 °C, 1.8 L of pentane. [c] 25 mL of 1-hexene. [d] n.m.: not measured. [e] No value.

ethene pressure) with M_w of 150 000 is 217 000 Pa s, which is clearly higher than the 107 000 Pa s obtained for polymer 21 with a similar M_w of 150 000 (polymerized at 10 bar). Going down to 2.5 bar in sample 27, M_w is increased to 205 000 and the MFR_{21} is only 1.2 g/10 min. Complex viscosity of this polymer could not be measured owing to the very slow relaxation of the material.

The response of the rheological behavior to the solvent was at first sight anomalous. Cat 2 produced long chain branched polymer both in toluene (sample 24) and in pentane (samples 21−23, 25−26). In contrast to this, Cat 4 polymers exhibited a different microstructure. Polymer 42, which was produced in pentane (in the presence of hydrogen) exhibited MWD 4.8, M_w of 116 000 and unexpected and peculiar dynamic moduli behavior indicative of long chain branching. Polymer 44, which was polymerized in toluene in the absence of H_2, exhibited a similar M_w, 120 000, but very narrow MWD of 2.0. Furthermore, the rheological behavior of this polymer indicated a linear chain structure, and the flow E_a was 28 kJ/mol. The peculiarities observed in the frequency dependence of the dynamic moduli of Cat 3, Cat 4, and Cat 5 polymers are discussed below.

***G′* and *G″* Curves.** Figure 5a shows the frequency dependence of the dynamic moduli of the linear polymer 12 produced with Cat 1 in toluene (judged to be linear on the basis of flow E_a). GPC analysis revealed a high M_w of 300 000 and a narrow MWD of 2.3 for the polymer. Parts b and c of Figure 5 show the moduli of polymers produced with the bridged catalysts. In the Cat 2 curves (Figure 5b), the contribution of the elastic modulus G' appears to be very large in comparison with that for the viscous modulus G''. Further, Figure 5c shows the curves for catalyst 4 and 5 polymers (produced in pentane solvent), where the storage modulus G' is parallel to the loss modulus G'' over the whole frequency region. In comparison with the curves of other polymers of similar M_w and MWD, the curves in Figure 5c are of somewhat peculiar curvature, which suggests the presence of some kind of network structure in the polymers.

Yet another interesting feature is the molecular weight and complex viscosity of the copolymers produced with Cat 3. The Cat 3 homopolymers yielded flow activation energy of 26 kJ/mol in pentane at both 10 bar (sample 31) and 2.5 bar ethene pressure (sample 33), so appearing linear in structure. Unexpectedly, the copolymers of this catalyst, Cat 3, exhibited a higher molecular weight and lower MFR_{21} than the corresponding homopolymers. This was seen at both high polymer yield (at 10 bar ethane pressure, polymer 32) and low polymer yield (at 2.5 bar ethene pressure, polymer 34). Figure 5d shows the dynamic moduli of a homopolymer and a copolymer produced with Cat 3. The homopolymer 33 exhibited values M_w 82 000, MWD 2.0, in GPC analysis, and copolymer 34 values M_w 113 000, MWD 2.8. As can be seen in the copolymer melt the elastic behavior dominated even at the lowest frequencies. This behavior again suggests a networklike structure, although no yield point typical for cross-linked materials[35] was evident in the complex viscosity curve.

We explain the long chain branching in the polymers in terms of incorporation of vinyl ended polymer chains in the polymerization. Other explanations, such as chain extension due to reacting vinyl bonds during sample preparation,[36] do not seem likely. Polymer stability during the dynamic rheological analysis was studied and found to be good. The polymerization and analytical results were reproducible, and the polymers suffered no changes in properties during the rheological analysis, as far as could be determined. Further, the dependence of molecular weight and complex viscosity on polymerization pressure (and polymerization time[33]) directly supports the assumption of in situ copolymerization. Yet another point is the varying behavior with the different catalyst structures; the unbridged $(n\text{-BuCp})_2ZrCl_2$ catalyst produced polymer with rheological behavior of

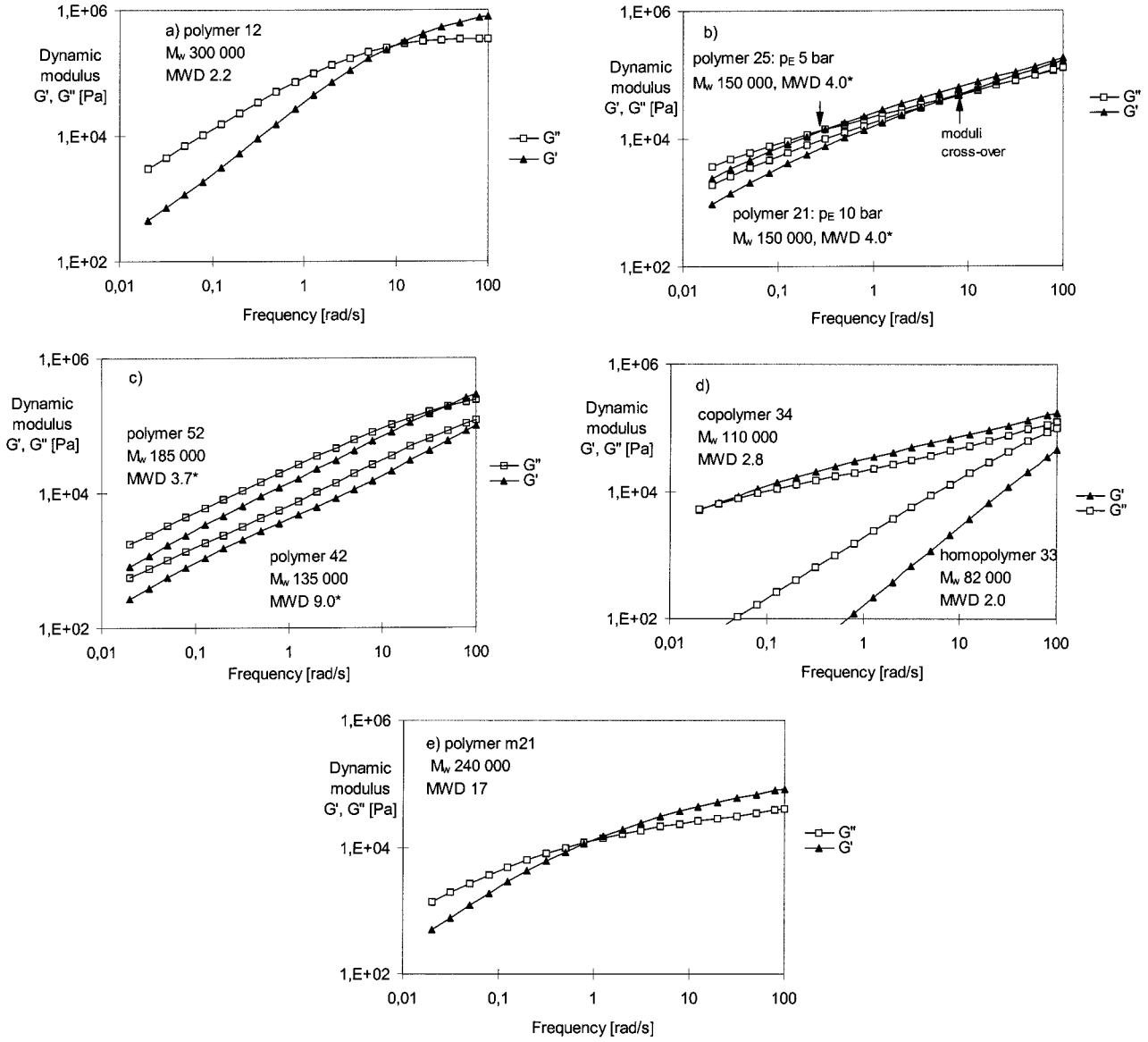

Figure 5. Dynamic storage modulus G' (filled symbols) and loss modulus G'' (open symbols) as a function of oscillation frequency at 190 °C: (a) polymer 12, produced with Cat 1; (b) Cat 2 polymer 25, polymerized at 5 bar ethene partial pressure, and polymer 21, polymerized at 10 bar; (c) Cat 5 polymer 52 and Cat 4 polymer 42 by catalyst 4; (d) Cat 3 ethene homopolymer 33 and ethene/1-hexene copolymer 34; (e) *meso*-Cat 2 polymer m21. An asterisk indicates M_w and MWD obtained by GPC−OLV analysis; otherwise they are obtained by GPC.

linear chains, whereas the bridged bisindenyl-substituted catalysts produced polymers that behaved consistent with low levels of long chain branching.

In copolymerization of vinyl-ended macromers with ethene, assuming only one vinyl end per molecule, no cross-links but only trifunctional branchpoints can occur.[9,37] Whereas incorporating one macromer in the chain produces a Y-like structure, the architecture becomes treelike if several macromers are incorporated in a single growing chain.[10] A treelike polymer with long enough branches topologically resembles a cross-linked, H-structure and could thus exhibit the relaxation behavior of a network. We note that catalysts 3, 4, and 5, which produced the most anomalous, networklike moduli behavior, also exhibited the strongest responses toward the comonomer 1-hexene.

Polymerization Process. As detailed above, the rheological behavior of the polymers showed them to vary from linear to long chain branched depending on the catalyst. Furthermore, distinctive LCB rheology was observed with structurally differing catalysts. Correlation among MFR_{21}, GPC-measured molecular weight and complex viscosity seemed virtually unique for each catalyst. Besides the selection of the catalyst, the polymerization conditions—ethene pressure, presence of hydrogen and comonomer and even the polymerization solvent—played a role in the long chain branch formation, as this was revealed in the rheological behavior. We now consider more closely the polymerization process itself.

For single site catalysts, a narrow MWD of 2 is predicted by the Schulz−Flory relation. Catalysts with several active sites produce heterogeneous polymers with broad and even multimodal MWD. Metallocene catalysts are generally agreed to possess only a single type of active site.[1] Termination of the growing chain in these systems may occur by chain transfer to the catalyst metal, to aluminum of the coactivator MAO, or to monomer. β-Hydrogen elimination to either monomer or catalyst metal leaves the chain ends with a vinyl

bond, which then can act as a macromer to produce long chain branching by copolymerization. β-Hydrogen elimination to the monomer is reflected in a molecular weight independent of ethene concentration. Earlier molecular dynamics studies have suggested β-hydrogen elimination to monomer to be the energetically most favorable alternative for bis-Cp structures.[38] Experimentally this has been observed for ethylene- and MeSi-bridged bisindenyl catalysts,[39] as well as for dimethylsilylene-bridged amidocyclopentadienyltitanium catalyst.[40] Very recently, Thorshaug et al.[41] reported both experimental results and density functional theory calculations for Cp_2ZrCl_2/MAO catalyst, supporting the dominance of the β-H elimination to monomer termination reaction with this catalyst. β-H elimination to the catalyst central metal rather than to monomer leads to strongly increasing molecular weight with ethene pressure. Experimental evidence for this mechanism has been found in α-methyl-substituted *ansa*-metallocenes[1] and with $Et(IndH_4)_2ZrCl_2$/MAO.[33,42]

The lowered molecular weight of the polymer in copolymerization[1,43] is readily explained by the facile β-H elimination after comonomer insertion, which gives a vinylidene end not capable of copolymerization in the chain. When long chain branching is formed by copolymerization, an increasing amount of short chain comonomer should act to reduce the degree of long chain branching. In fact, although in linear chains increasing comonomer content increases the polymer flow E_a,[5,32] in long chain branched copolymers prepared by the $Et(Ind)_2ZrCl_2$/MAO catalyst, higher comonomer content results in decreased E_a.[33] Nevertheless, as discussed above, the rheological behavior indicates a more complex structure of the chain in some of the ethene/1-hexene copolymers than in the homopolymers. While this behavior was most clearly seen with Cat 3, it was also present in Cat 2 and Cat 4 and even in EBIZ polymers when the comonomer content was very low. These findings are in line with the observations of Harrison et al.,[6] who reported the LCB incidence to be higher in ethene/1-hexene copolymerization than in ethene homopolymerization with the EBIZ catalyst.

Polymerization conditions of low ethene concentration and high polymer (vinylic end) concentration should favor the macromer incorporation.[2] Presumably both of these conditions are met in the semibatch slurry polymerization at relatively low ethene partial pressures and long polymerization times. In slurry process, the particle forming process[44] in the homogeneous metallocene (ethene homo-) polymerizations is controlled by monomer diffusion. Similarly, the rate of macromonomer insertion should be limited by the rate at which the macromonomer can diffuse through the polymer encapsulated active site.[2] Although recent modeling studies speak for macromonomer reinsertion at the catalyst center where it was originally formed,[45] the cross-linking observed in ethene/diene copolymerizations[46] appears to support some diffusion of the chains in the slurry particles.

Kinetics modeling studies indicate broadening MWDs with increasing degree of long chain branching.[9,10] Another source of broadening of the MWD is the mass and heat transfer limitations possibly present in a semibatch slurry polymerization. With very active polymerization catalysts, mass transfer limitations, specifically the rate of ethene solubility at the gas−liquid interface, may become the limiting step. Furthermore, heat transfer properties have been shown to be different in disperse homopolymerizations than in partly or completely solution copolymerizations.[47] If reactor fouling occurs, the situation becomes even more complicated: diffusion of ethene and hydrogen to the catalyst active center is retarded and heat transfer from the exothermic polymerization reaction to the medium becomes more restricted. Linear α-olefin comonomers in copolymerizations contribute through physical and chemical effects. Comonomers enhance polymer solubility and may affect initiation and propagation rates.[48,49] Not only does the MWD become broader as a result of mass and heat transfer limitations but also the comonomer distribution does.[50,51]

The polymerizations reported here were not kinetically, but diffusion-controlled at the highest ethene pressures. Stirring rate was found to affect the ethene flow rate during polymerization, which is an indication of mass transfer limitation from the gas phase to the liquid phase. In slurry polymerization, the concentration of ethene at the catalyst site is unknown. This is unfortunate, since monomer concentration is of great importance to the polymer properties, as demonstrated above. Local variations in ethene concentration in the reactor could occur if fouling takes place, or variation could occur even in single slurry particles if the polymer for some reason should form a tight shell around the active site. In an environment with local variations in ethene concentration, a catalyst capable of producing vinyl ended chains and copolymerizing them could give rise to complex branches-on-branches topologies.

Although mass transfer effects may have contributed to the properties of the polymers, they are not the only cause of them. We note once again that, under similar polymerization conditions in pentane (and similar polymer yields), the $(n\text{-butCp})_2ZrCl_2$ catalyst produced polymer with rheological behavior typical of highly linear chains, while each of the bridged catalysts produced a distinctive LCB behavior. Moreover, the broadened molecular weight distributions and the LCB rheology, even the networklike behavior of the copolymers, were produced also at low ethene pressures, where the yields were very low and mass transfer limitations should have been at minimum. Furthermore, catalysts $Et(Ind)_2ZrCl_2$ and the siloxy-substituted Cat 2 produced relaxation behavior indicative of long chain branched structure in both homo- and copolymerizations, in both solvents, at every polymerization pressure studied.

Conclusions

In semibatch ethene homopolymerizations and copolymerizations with 1-hexene carried out with bridged and unbridged homogeneous metallocene catalysts, we observed the following points:

1. In the polymers produced with 1- and 2-siloxy-substituted $Et(Ind)_2ZrCl_2$/MAO (EBIZ-type) and MeSi-$(C_5Me_4)(N\text{-}t\text{-Bu})TiCl_2$/MAO catalysts, the complex viscosity at low frequency was very high and the shear thinning of the viscosity was steep. This behavior was unexpected given the M_w and narrow MWD values obtained in GPC analysis and indicates the presence of very slowly relaxing, high molecular weight species in the polymers. The unbridged $(n\text{-butCp})_2ZrCl_2$/MAO catalyst, in turn, produced polymers with rheological behavior typical of straight chain polymers. The *meso* form of one of the EBIZ-type catalysts gave a broad

MWD and, accordingly, a simple shear thinning behavior.

2. A low value of flow activation energy, 26 kJ/mol, was obtained for the (n-butCp)$_2$ZrCl$_2$/MAO catalyst polymer, indicating a very linear HDPE structure. Flow activation energies were high for the polymers produced with the EBIZ-type and dimethylsilylene-bridged amidocyclopentadienyltitanium catalysts— even as high as those of LDPE, over 50 kJ/mol—but the GPC-on-line viscometry results indicated less branching than in LDPE.

3. In the polymers with elevated flow E_a, the proportion of elastic modulus G' was large relative to the viscous response G″. In some of the polymers, the elastic modulus G' followed the viscous modulus G'' over the whole frequency region.

4. The relationships between M_w, MFR at 21 kg load, and the dynamic rheological behavior seemed to be distinctive for each catalyst.

5. We explain the findings in terms of different, very low contents of long chain branches in the polymers. Moreover, these long chain branches may be further branched. Branches-on-branches structures may form through copolymerization of more than one vinyl-ended macromer in the chain. Factors favoring this behavior are the good copolymerization ability of the catalyst and the existence of termination paths producing vinyl ends in the polymers.

6. The polymerization conditions contribute to the long chain branching behavior. Low ethene pressure favors macromer insertion, whereas comonomer and hydrogen decrease the amount of vinyl-ended chains, and thus they should reduce the probability of complex structures. However, some of the copolymers of low comonomer content appeared to be more long chain branched than were the homopolymers.

7. The role of the polymerization conditions is emphasized with highly active polymerization catalysts. Mass and heat transfer limitations occur easily, and precise control of the polymerization becomes difficult. Under suitable conditions, low contents of complex, branches-on-branches structures may form, which then manifest themselves in the rheological behavior of the polymer. Thus, both the catalyst and the process conditions contribute to the long chain branch formation and to the distribution of the branches. This conclusion also implies that not the content but the structure (distribution) of the long chain branches is the parameter to be controlled. Evidently, the factors most likely to influence the structure are the amounts of comonomer and hydrogen.

Acknowledgment. We warmly thank Sari Wahrman for the polymerizations, Heidi Bryntesen, Borealis AS, for the GPC−OLV measurements and Lambda Polynom and Wyatt Technologies for the GPC−LS measurements. Funding for this project was received from the Technology Development Centre, Helsinki, Finland, and Borealis Polymers Oy.

References and Notes

(1) Brintzinger, H.-H.; Fischer, D.; Mülhaupt, R.; Rieger, B.; Waymouth, R. M. *Angew. Chem., Int. Ed. Engl.* **1995**, *34*, 1143−1170.

(2) (a) Hamielec, A. E.; Soares, J. B. P. *Prog. Polym. Sci.* **1996**, *21*, 651−706. (b) Soares, J. B. P.; Hamielec, A. E. *Macromol. Theoy Simul.* **1996**, *5*, 547−572.

(3) Shiono, T.; Moriki, Y.; Soga, K. *Macromol. Symp.* **1995**, *97*, 161−167.

(4) Vega, J. F.; Muñoz-Escalona, A.; Santamaría, A.; Muñoz, M. E.; Lafuente, P. *Macromolecules* **1996**, *29*, 960−965.

(5) Vega, J. F.; Santamaría, A.; Muñoz-Escalona, A.; Lafuente, P. *Macromolecules* **1998**, *31*, 3639−3647.

(6) Harrison, D.; Coulter, I. M.; Wang, S.; Nistala, S.; Kuntz, B. A.; Pigeon, M.; Tian, J.; Collins, S. *J. Mol. Catal. A* **1998**, *128*, 65−77.

(7) Howard, P.; Maddox, P. J.; Partington, S. R. BP Chemicals Ltd. EP 0 676 421 A1.

(8) Malmberg, A.; Kokko, E.; Lehmus, P.; Löfgren, B.; Seppälä, J. V. S. *Macromolecules* **1998**, *31*, 8448−8454.

(9) Zhu, S.; Li, D.; Zhou, W.; Crowe, C. M. *Polymer* **1998**, *39*, 5203−5208.

(10) Zhu, S.; Li, D. *Macromol. Theory Simul.* **1997**, *6*, 793−803.

(11) Leino,R.; Luttikhedde, H. J. G.; Lehmus, P.; Wilén, C−E.; Sjöholm, R.; Lehtonen, A.; Seppälä, J. V.; Näsman, J. H. *Macromolecules* **1997**, *30*, 3477−3483.

(12) Lehmus, P.; Kokko, E.; Härkki, O.; Leino,R.; Luttikhedde, H. J. G.; Näsman, J. H.; Seppälä, J. V. *Macromolecules* **1999**, *32*, 3547−3552.

(13) Randall, J. C. *J. Macromol. Sci. Rev. Macromol. Chem. Phys.* **1989**, *C29*, 201−317.

(14) Haslam, J.; Willis, H. A.; Squirrel, D. C. M. *Identification and Analysis of Plastics*, 2nd ed.; Iliffe Books: London, 1972.

(15) Rudin, A.; Pang, S. *J. Appl. Polym. Sci.* **1992**, *46*, 763−773.

(16) Lachtermacher, M.; Rudin, A. *J. Appl. Polym. Sci.* **1995**, *58*, 2077−2094.

(17) Kulin, L. I.; Meijerink, N. L.; Starck, P. *Pure Appl. Chem.* **1988**, *60*, 1403−1415.

(18) Raju, V. R.; Smith, G. G.; Marin, G.; Knox, J. R.; Graessley, W. W. *J. Polym. Sci.* **1979**, *17*, 1183−1193.

(19) Graessley, W. W. *Macromolecules* **1982**, *15*, 1164−1167.

(20) (a) Mavridis, H.; Shroff, R. *J. Appl. Polym. Sci.* **1993**, *49*, 299−318 (b) Mavridis, H.; Shroff, R. *J. Appl. Polym. Sci.* **1995**, *57*, 1605−1626.

(21) Harrell, E. R.; Nakajima, N. *J. Appl. Polym. Sci.* **1984**, *29*, 995−1010.

(22) (a) Lachtermacher, M.; Rudin, A. *J. Appl. Polym. Sci.* **1995**, *58*, 2433−2449. (b) Lachtermacher, M.; Rudin, A. *J. Appl. Polym. Sci.* **1996**, *59*, 1213−1221.

(23) Bersted, B. H. *J. Appl. Polym. Sci.* **1985**, *30*, 3751−3765.

(24) Raju, V. R.; Rachabudy, H.; Graessley, W. W. *J. Polym. Sci.* **1979**, *17*, 1223−1235.

(25) Graessley, W. W.; Raju, V. R. *J. Polym. Sci., Polym. Symp.* **1984**, *71*, 77−93.

(26) Carella, J. M.; Gotro, J. T.; Graessley, W. W. *Macromolecules* **1986**, *19*, 659−667.

(27) Hughes, J. K. *SPE ANTEC Tech. Pap.* **1984**, *29*, 306−309.

(28) Mavridis, H.; Shroff, R. *Polym. Eng. Sci.* **1992**, *32*, 1778−1791.

(29) Wasserman, S. H.; Graessley, W. W. *Polym. Eng. Sci.* **1996**, *36*, 852−861.

(30) Kim, Y. S.; Chung, C. I.; Lai, S. Y.; Hyun, K. S. *J. Appl. Polym. Sci.* **1996**, *59*, 125−137.

(31) Hatzikiriakos, S. G.; Kazatchkov, I. B.; Vlassopoulos, D. *J. Rheol.* **1997**, *41*, 1299−1315.

(32) Mehta, A. K.; Speed, C. S.; Canich, J. A. M.; Baron, N.; Folie, B. J.; Sugawara, M.; Watanabe, A.; Welborn, H. C., Jr. Exxon Chemicals, Int. Pat. WO 96/12744.

(33) (a) Kokko, E.; Lehmus, P.; Malmberg, A.; Löfgren, B.; Seppälä, J. V. Metallocene catalyzed polyethenes with improved rheological properties, *Dechema Monographs series*; Wiley-VCH: Berlin, 1998; Vol. 134, pp 115−124. (b) Kokko, E.; Malmberg, A.; Lehmus, P.; Löfgren, B.; Seppälä, J. V. Submitted for publication in *J. Polym. Sci.* (1999).

(34) Suhm, J.; Schneider, M. J.; Mühlhaupt, R. *J. Mol. Catal. A* **1998**, *128*, 215−227.

(35) Nakajima, N. *Polym. Int.* **1995**, *36*, 105−116.

(36) Foster, G. N.; Wasserman, S. H.; Yacka, D. J. *Angew. Macromol. Chem.* **1997**, *252*, 11−32.

(37) Sugawara, M. *SPO'94* **1994**, 39−50.

(38) Woo, T. K.; Margl, P. M.; Ziegler, T.; Blöchl, P. E. *Organometallics* **1997**, *16*, 3454−3468.

(39) Spaleck, W.; Küber, F.; Winter, A.; Rohrmann, J.; Bachmann, B.; Antberg, M.; Dolle, V.; Paulus, E. F. *Organometallics* **1994**, *13*, 954−963.

(40) Soga, K.; Uozumi, T.; Nakamura, S.; Toneri, T.; Teranishi, T.; Sano, T.; Arai, T. *Macromol. Chem. Phys.* **1996**, *197*, 4237−4251.

(41) (a) Thorshaug, K.; Støvneng, J. A.; Rytter, E.; Ystenes, M. *Macromolecules* **1998**, *31*, 7149−7165. (b) Thorshaug, K.; Rytter, E.; Ystenes, M. *Macromol. Rapid Commun.* **1997**, *18*, 715−722.
(42) Leclerc, M. K.; Brintzinger, H. H. *J. Am. Chem. Soc.* **1996**, *118*, 9024−9032.
(43) Lehtinen, C.; Starck, P.; Löfgren, B. *J. Polym. Sci.* **1997**, *35*, 307−318.
(44) Herrmann, H−F.; Böhm L. L. *Polym. Commun.* **1991**, *32*, 58−61.
(45) Margl, P.; Deng, L.; Ziegler, T. *Organometallics* **1998**, *17*, 7**,** 933−946.
(46) Pietikäinen, P.; Seppälä, J. V.; Ahjopalo, L.; Pietilä, L. *Eur. Polym. J.*, in press (1998).
(47) (a) Lahti, M.; Koivumäki, J.; Seppälä, J. V. *Angew. Macromol. Chem.* **1996**, *236*, 139−153. (b) Lahti, M.; Koivumäki, J.; Seppälä, J. V. *Angew. Macromol. Chem.* **1996**, *236*, 155−167.
(48) Koivumäki, J. Ph.D. thesis, Helsinki University of Technology, 1994.
(49) Cruz, V. L.; Muñoz-Escalona, A.; Martinez-Salazar, J. *J. Polym. Sci.* **1998**, *36*, 1157−1167.
(50) Atiquillah, M.; Hammawa, H.; Akhtar, M. N.; Khan, J. H.; Hamid, H. *J. Appl. Polym. Sci.* **1998**, *70*, 137−147.
(51) Lehmus, P.; Härkki, O.; Leino, R.; Luttikhedde, H. J. G.; Näsman, J.; Seppälä, J. V. *Macromol. Chem. Phys.* **1998**, *199*, 1965−1972.

MA9907136